**TRANSACTIONS OF THE INSTITUTE OF AVIATION** ISSN 0509-6669
**218**, pp. 86-96, Warsaw 2011

# EFFECTIVENESS OF AN INVERTED-V-SHAPED CONTROL SURFACES OF A GYROPLANE AT LOW SPEED AND HIGH-ANGLES-OF-ATTACK

Janusz Sznajder

*Institute of Aviation*

*Abstract*

*An inverted-V-shaped control surface configuration has been applied in a design of a light gyroplane. Two variants of the inverted-V-shaped control surfaces have been investigated in the present work: all moving version and stabilizer-rudder solution with 70% chord rudder. The focus of the investigation is on high angle of attack characteristics important for low-speed, short-distance or power-off landing approach.*

## INTRODUCTION

Main benefits of application of a V-shaped tail surface configuration in light aircraft are structural simplicity and savings on manufacture costs. The drawback of this solution is slightly more complicated control system, involving elements making it possible to execute symmetric and asymmetric movements of control surfaces. Similar motivations are important also in application of this type of tail surfaces in the design of a light gyroplane. In a gyroplane the role of the tail surfaces differ slightly from their role in a fixed-wing aircraft. The elevator is no longer the main instrument for longitudinal control, since this action is performed by the deflection of the rotor shaft in the symmetry plane. The elevator may, however, be used for horizontal trim. The horizontal stabilizer plays also an important role in preventing the 'power push-over' phenomenon and damping longitudinal oscillations of the fuselage. The 'power push-over' phenomenon may occur, when rotor angular velocity and lift suddenly decrease and the gyroplane is subject to unbalanced pitching moment from the propeller, if the propeller thrust line is not aligned with the gyroplane C.G (Figure 1). Horizontal tail then significantly reduces pitch velocity, enabling the pilot to react to this situation by deflecting the rotor shaft and changing blade pitch angle, or by supplying the torque to rotor from engine, if possible. The vertical tail is necessary to provide directional stability, as in fixed-wing aircraft. Unlike a fixed-wing aircraft, a gyroplane can safely perform turns without rudder deflection, using instead deflection of rotorhead in the Y-Z plane. The gyroplane then performes a sideslip movement and then the fuselage aligns with the new flight direction due to its directional stability. However, in some phases of flight, such as short-distance landing especially with side-wind, an efficient directional control is necessary for maintaining the direction of flight. Since there is no tail rotor, in contrast

to helicopters, control of the yaw angle must be executed using rudder.For a classical tail-surface system, as well as for the V-shaped tail surfaces the requirements for aicraft controlability at low speed lead to increasing of the control surface area. This is difficult in a gyroplane design, due to the presence of the rotor on a deflectable shaft above the fuselage. One way of dealing with with this constraint is the application of an inverted-V-shaped control surfaces. The way of providing high effectiveness of the control surfaces is then the application of all-moving control surfaces, or increasing the rudder surface of a two-element tail surface (elevator + rudder) well above 50 percent of chord. This choice has been investigated in the present work.

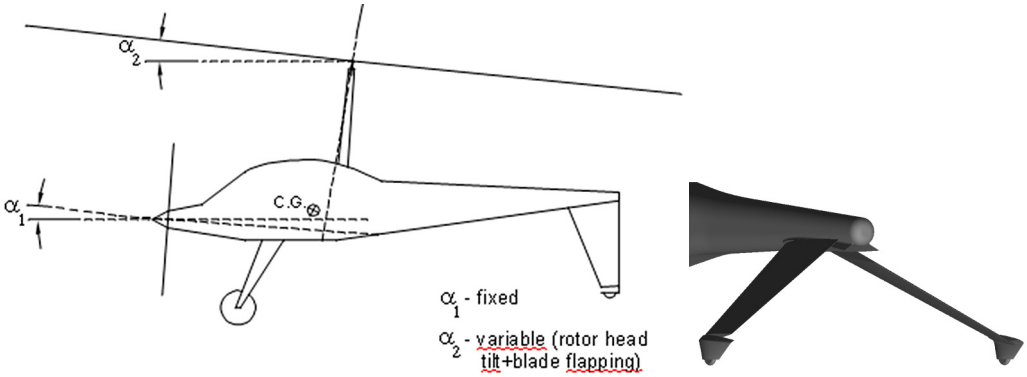


Figure 1. General view of a gyroplane with a tractor-type power system and inverted-V shaped tail surfaces

**Two-dimensional analysis**

Two-dimensional analysis was aimed at determination of maximum lift coefficient, and derivatives of lift and hinge moment with respect to angle of rudder deflection for selected configurations which included an all-moving section (single airfoil) and several rudder/airfoil-chord proportions. The airfoil selected was NACA0012 – typical airfoil applied for control surfaces. The airspeed for the test was set at 50km/h, approximately the take-off velocity of a typical light gyroplane. The Reynolds number was set at 608500 which corresponds to tail chord of 0.64m. The detailed proportions of rudder/chord ratio and the positions of the rotation axis of the moving element are shown in Table 1.

Table1. Geometric data of the investigated rudder-airfoil chord ratios

| rudder/chord ratio | $x_{axis}/c$ |
|---|---|
| 100% - all moving tail surface | 20% |
| 70% | 35.926% |
| 60% | 45.545% |
| 50% | 54.943% |

The aerodynamic characteristics of the presented rudder configurations were determined using Fluent solver, using k-omega-SST turbulence model [1,2] on a grid of 24000 elements. The k-omega-SST turbulence model is considered appropriate for modeling of viscous flows at low Reynolds numbers. In the computational grid the main element-rudder junction was sealed. This is a justified procedure for narrow slots in the model, accelerating the convergence of the solution. The computed $c_L$-$\delta_{rudder}$ characteristics are shown in Fig. 2.

It follows from Fig. 2 that $c_{L\,max}$ of rudder/airfoil chord ratios greater than 50% are higher than for all-moving control surface. This may be explained by the chordwise distribution of pressure coefficient $c_p$ over the investigated NACA0012 airfoil. A deflected rudder of rudder/chord ratio more than 50% modifies significantly $c_p$ distribution in the front part of the airfoil, increasing the length of the low-pressure area (Figures 3 and 4).

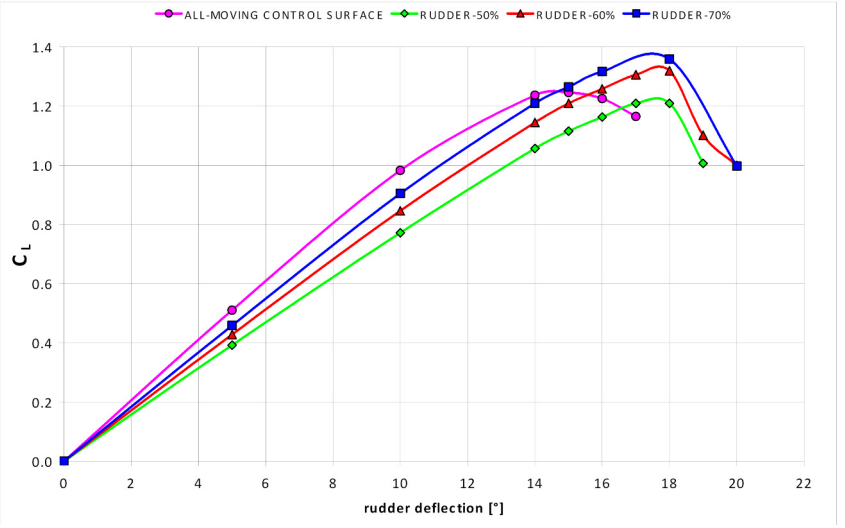


Figure 2. $C_L$ - $\delta_{rudder}$ characteristics for different rudder/airfoil chord ratios

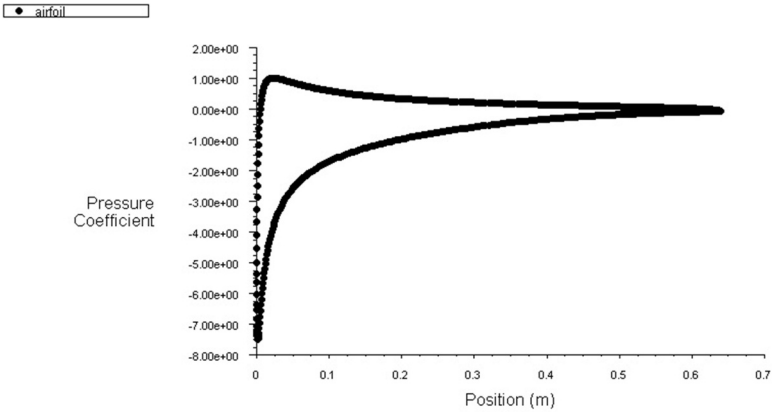


Figure 3. Distribution of pressure coefficient on NACA 0012 airfoil at α=14 deg (near $\alpha_{CL\,max}$)

As a measure of the effectiveness of a rudder a nondimensional coefficient $\alpha_\delta$ - angle of attack effectiveness, (ratio of derivatives $c_{L\alpha}$ and $c_{L\delta}$) is frequently used[3]. This coefficient, determined for the rudder/airfoil chord ratios presented in Table 1 is shown in Fig. 5. The data shows, that rudder/airfoil chord ratios of 60-70% are very effective at generating lift force, producing required lift coefficient at moderately larger deflection angle (10-17%) than all-moving control surface.

This characteristic and others, including $c_{Lmax}$, $\dfrac{\partial c_{m\ \mathrm{hinge}}}{\partial \delta_{\mathrm{rud}}}$, $c_{m\ \mathrm{hinge\ max}}$ are shown in Table 2.

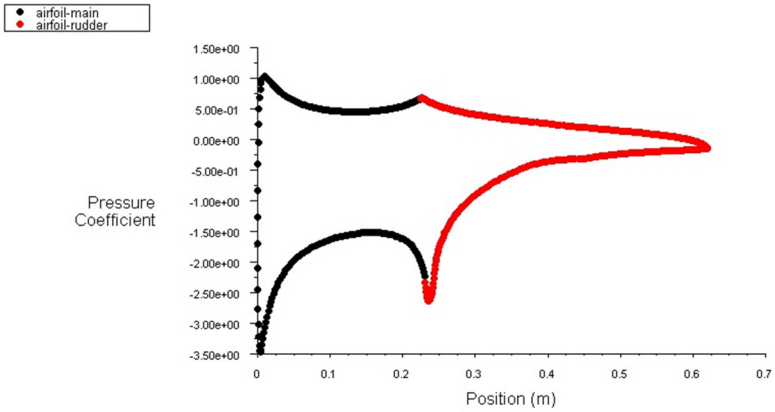


Figure 4. Distribution of pressure coefficient on NACA 0012 airfoil with 70% c rudder at rudder deflection $\delta_r = 18°$ (near $\delta_{r\,CL\,max}$)

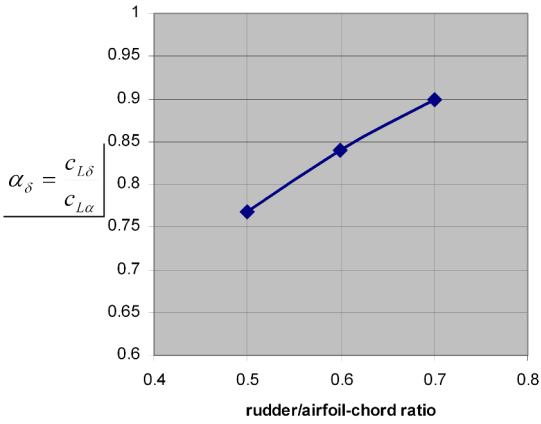


Figure 5. Angle of attack effectiveness for the investigated rudder-airfoil chord ratios

Table 2. Results of two-dimensional flow analysis of the investigated rudder-airfoil chord ratios

| rudder/airfoil chord | $x_{axis}$/airfoil chord | $\delta_{rud\,CL\,max}$ [°] | $c_{L\,max}$ | $\alpha_\delta = \frac{c_{L\alpha}}{c_{L\delta}}$ | $\frac{\partial c_{m\,hinge}}{\partial \delta_{rud}}$ | $c_{m\,hinge\,max}$ |
|---|---|---|---|---|---|---|
| 100% | 0.20 | 15 | 1.242 | 1.0 | -0.275 | -0.047 |
| 50% | 0.549 | 18 | 1.218 | 0.769 | -0.147 | -0.039 |
| 60% | 0.455 | 18 | 1.321 | 0.840 | -0.234 | -0.061 |
| 70% | 0.359 | 18 | 1.360 | 0.898 | -0.357 | -0.0898 |

## THREE-DIMENSIONAL ANALYSIS

### Low angles of attack, effect of propeller wake

Three-dimensional computations were performed for an all-flying tailplanes with sweep angle in the X-Y plane of 20°, sweep in XZ-plane of 34°, dihedral of -30°, taper of 0.465, span of 2.94m and surface area of 1.841m$^2$. The primary function of the tailpanes is providing direc-

tional stability and controllability in yaw (using antisymmetric deflections with respect to X-Z plane), as well as trim corrections for logitudinal balance (using symmetric deflections with respect to X-Z plane). The secondary function of the tailplanes consists in working as the rear undercarriage.

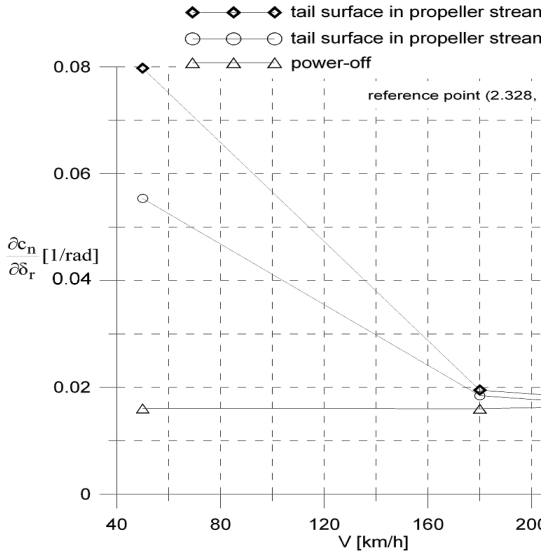


Figure 6. Derivative of yawing moment due to rudder deflection in cruise conditions including effects of propeller stream

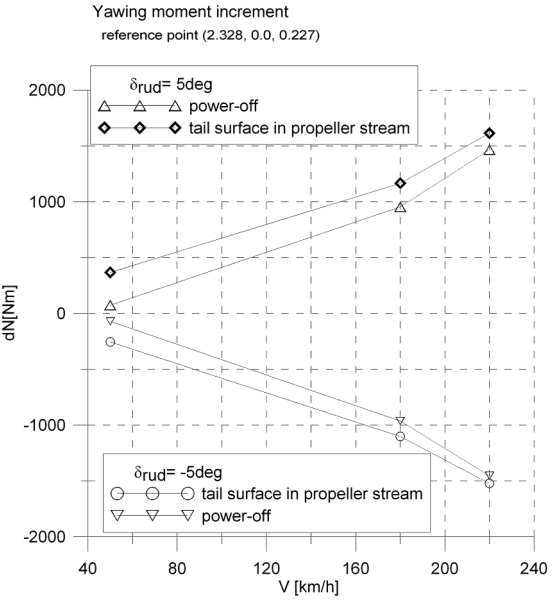


Figure 7. Increment of yawing moment due to rudder deflection in cruise conditions including effects of propeller stream

The basic characteristics expressing the effectivenesss of the tail surfaces – derivatives of yawing moment coefficient with respect to the angle of surface deflection and yawing moment

increment due to angle of surface deflection are shown in Figures 6 and 7. The surface deflection angle was 5°. The computations were performed using Fluent solver for cases with and without working propeller. The effect of propeller stream was modeled using the fan boundary condition on the grid zone representing the propeller. The distribution of pressure jump along fan radius and circumferential velocity distribution on the fan surface were set based on simulation of the working propeller using Virtual Blade Model [4] The propeller thrust was set at 2.2 kN at speed of 50 km/h and 1.47kN at 180 and 220 km/h. It is clearly visible that propeller stream has a favourable effect on the $c_{n\delta r}$ derivative at low speeds, increasing significantly its value. The large increase of the value of the derivative at low speed is due to the large increase of dynamic pressure in the tail region at low speed. Yawing moment increment in the propeller effect is greater if the rudder is deflected in the direction of the coils of the propeller wake. The distribution of the flow velocity in a vertical plane just ahead of the vertical tail, induced by the propeller for gyroplane standing on the ground, is shown in Figure 8. The distribution is assymetric, with higher flow velocities around the left element. The propeller thrust was set at 2.2 kN. The aerodynamic coeffficients were calculated using as reference the rotor disk surface area and rotor radius equal 4.2m.

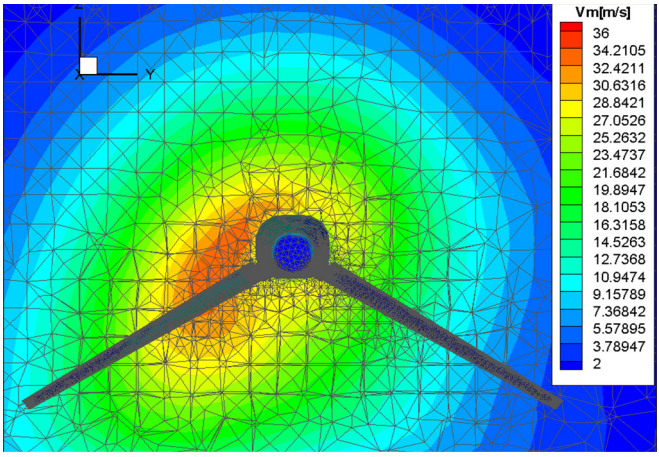


Figure 8. Distribution of propeller axial velocity in a plane just ahead of tail surface root for a gyroplane standing on the ground

**Effectiveness of tail surfaces at high angles of attack**

A specific feature of gyroplanes is their ability to perform short-distance landing, executed with steep descent. Such landing is also performed in emergency situations in power-off flight. Because of absence of tail-rotor which ensures directional stability and contollability of helicopters, gyroplanes must rely on the effectivness of tail control surfaces. Effectiveness of control surfaces must be ensured especially for conditions of low forward speed and high fuselage angles of attack, as these are typical conditions of steep low-speed, power-off landing.

Shown in Figure 9 is the derivative of yawing moment with respect to rudder deflection for the range of fuselage angle of attack from 0 to 16 deg. The computations were performed for the basic design of two all-moving, single-element surfaces. The propeller effect was not included in the computations in order to simulate conditions of power-off landing. The characteristic result for this configuration is its decreasing effectiveness at high angles of attack and change of sign of the $c_{n\delta r}$ derivative at approximately 12.5 deg angle of attack for the basic

design of all-flying tailplanes. This reverse action of the control surfaces is of course unaccteptable. The cause of this phenomenon is flow separation developing at the surface with higher deflection. This is explained in detail in Figures 10 and 11.

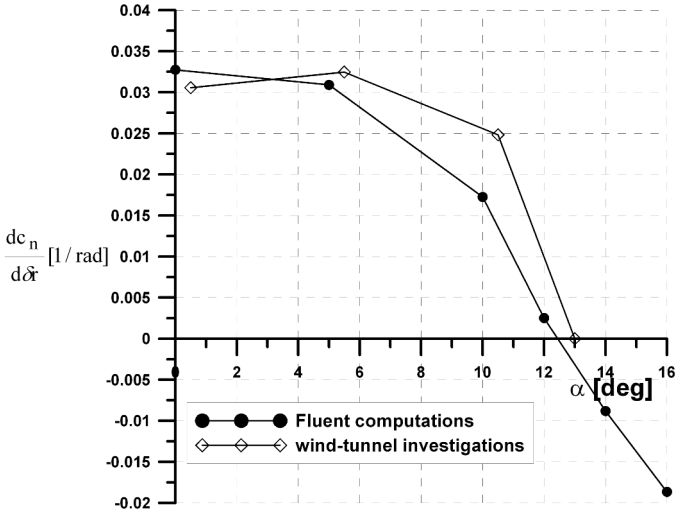


Figure 9. Change of $c_{n\delta r}$ derivative with angle of attack for all-moving control surfaces

Presented in Figure 10 is the side-force derivative with respect to the rudder deflection $\frac{\partial c_Y}{\partial \delta r}$ versus fuselage angle of attack. Along the curve for the total value (sum over the left and right element) shown are separate curves for the right and left element. The reason for the reverse action of tail surfaces may be found by analyzing the curves for individual elements. The derivative was determined assuming positive deflection of the right element (increasing its angle of attack) and negative deflection of the left element (decreasing its angle of attack).

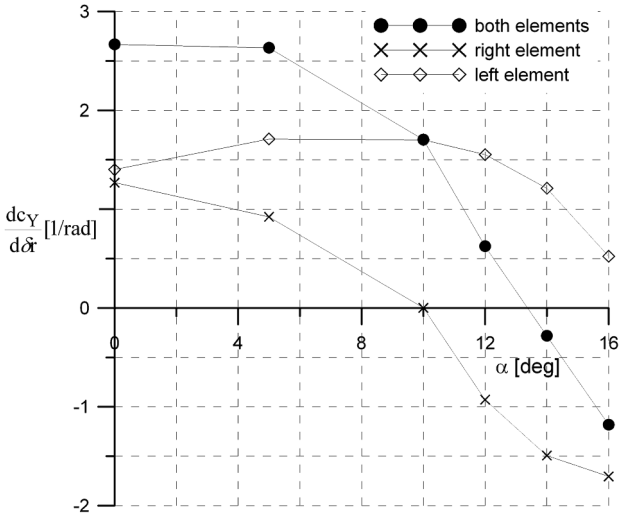


Figure 10. Change of $c_{Y\delta r}$ derivative with angle of attack for complete all-flying surface tail unit and for each element separately

The value of the $c_{Y\delta r}$ derivative for the right element reaches 0 at approximately α=10° and becomes negative, while for the left element remains positive. This is explained by the developing flow separation on the right tail surface at angle of attack above 10° (Figure 11). Increasing the angle of attack on the right element above $\alpha_{crit}$ leads to decreasing of the lift force and the side force on this element. The decrease of lift on the right element, due to flow separation is higher in magnitude than the decrease of lift on left element where the angle of attack was lowered. As a result, the total force changes direction from right to left. The change of the yawing moment is then from positive to negative, as the yawing moment is generated by the side force on the tail surfaces.

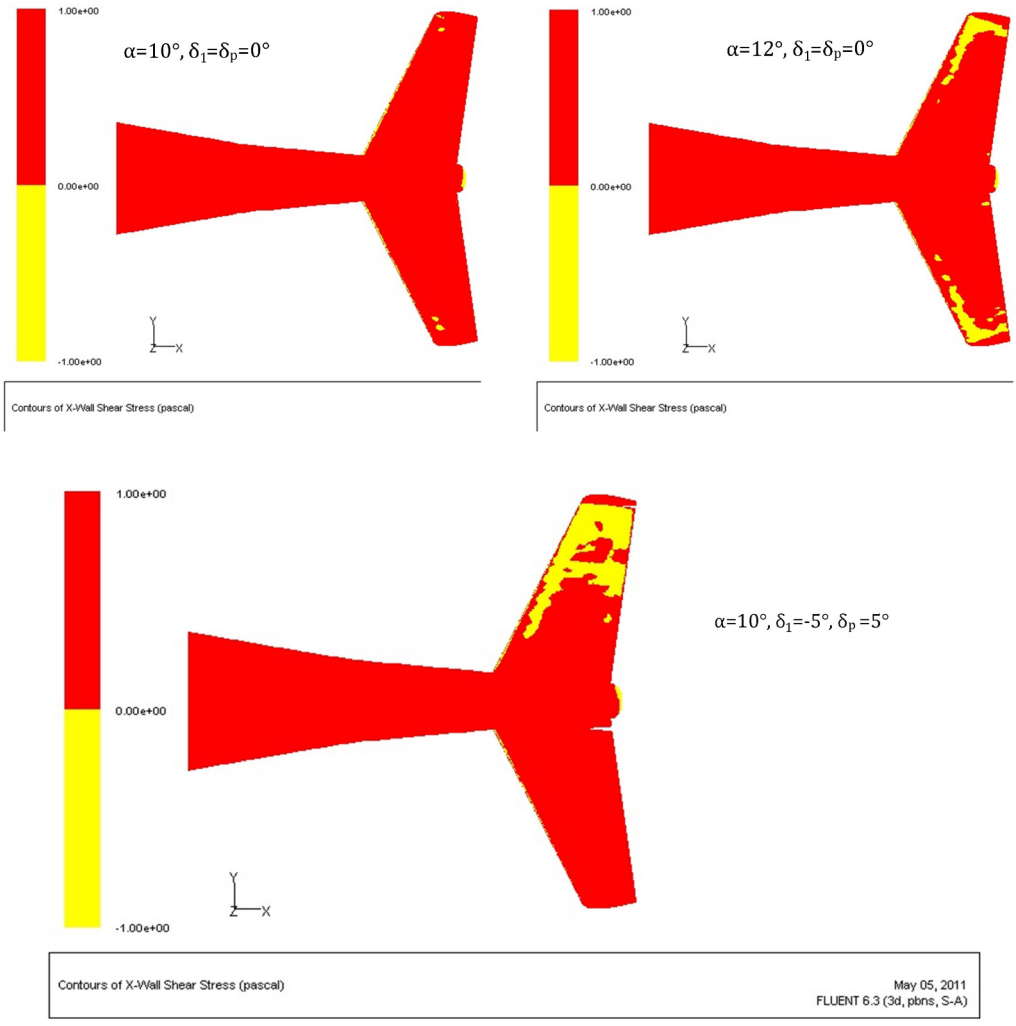


Figure 11. Contours of wall shear stress coefficient in x-direction for the all-moving tail surface configuration. Color maps with two values in order to display the extent of the separated area (positive x-shear stress - red color – area of attached flow, negative x-shear stress - yellow color – area of separation)

Computations of the effectiveness of tail surfaces at high fuselage angles of attack were performed also for the split tailplanes with 70% chord rudder. The results of the computations are presented in Figures 12 and 13. The results show an improvement of the effectiveness of the control surfaces in a sense that the reverse action occuring for all moving variant is eliminated. The value of the $c_{n\delta r}$ derivative, however, still decreases significantly for fuselage angle of attack higher than α=10°.

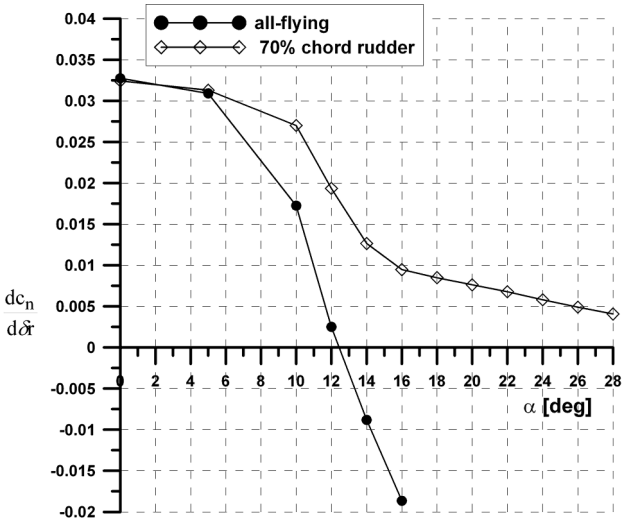


Figure 12. Comparison of the derivative of yawing moment with respect to rudder deflection for a gyroplane with all-moving, single-element tailpanes and stabilizer-rudder configuration

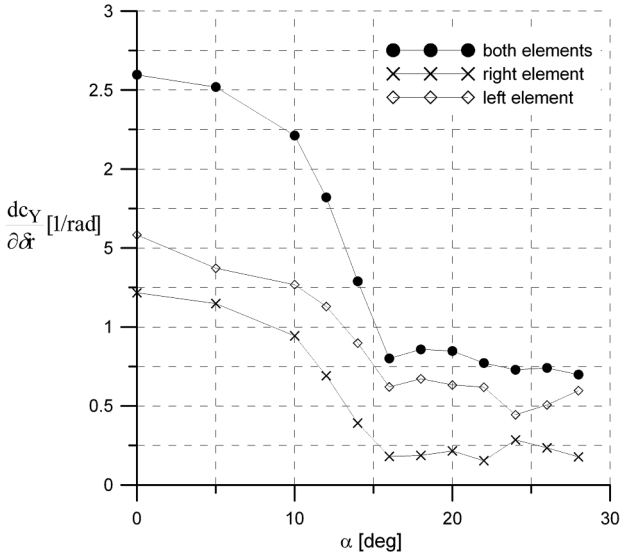


Figure 13. Change of $c_{Y\delta r}$ derivative with angle of attack for complete tail unit and for each element of the elevator-rudder configuration separately

The change of derivative of side-force coefficient with angle of attack for the split tailplanes, including data for the left and right element separately is shown in Figure 13. In this case the derivative remains positive on both elements. The distribution of X-wall shear stress on both el-

ements for the case with deflected rudders is shown in Figure 14. It can be seen, that with increasing the fuselage angle of attack separation develops on both elements. This explains the drop of effectiveness of the tail unit at fuselage angles of attack over 10° and also indicates that both elements, left and right, are working in similar conditions. It can be seen also, that grater increase of side force occurs on the left element with rudder deflected negative towards the flow (decreasing local angle of attack).

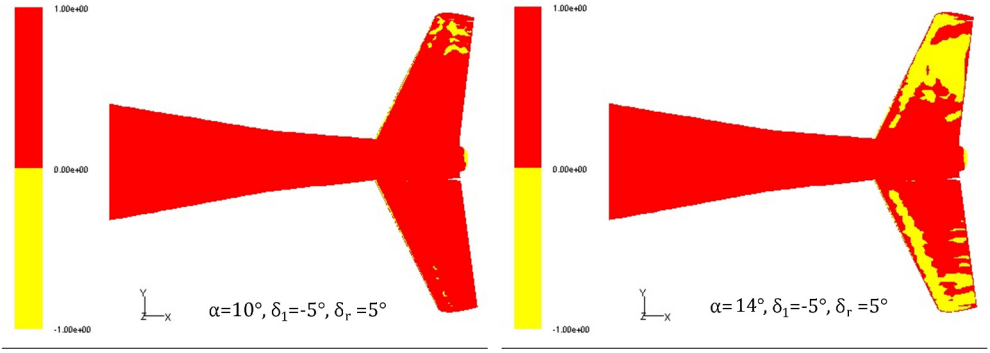


Figure 14. Contours of wall shear stress coefficient in x-direction
for the elevator-rudder tail surface configuration

Contributions of each tail component part (fixed and moving) to the value of the derivative at fuselage angle of attack α=5° and 14° are shown in Table 3. It can be seen, that in the presence of flow separation more effective are elements for which deflection of the rudder decreases local angle of attack (left stabilizer and rudder are both producing increase of side force), and on the right side, with increasing local angle of attack, increase of side force is generated mainly on the rudder. At lower fuselage angle of attack the contributions of the left and right elements are more balanced.

Table 3. Contributions of elements of the split tailplane configuration
to the derivative of side-force due to rudder deflection

| fuselage angle of attack | $\frac{\partial c_Y}{\partial \delta r}$ total | left elevator + left rudder | left elevator | left rudder | right elevator + right rudder | right elevator | right rudder |
|---|---|---|---|---|---|---|---|
| 5 | 2.5193 | 1.3713 | 0.7877 | 0.5836 | 1.1480 | 0.7517 | 0.3963 |
| 14 | 1.2889 | 0.8978 | 0.4133 | 0.4845 | 0.3911 | 0.0617 | 0.3294 |

## CONCLUSIONS

- The original solution of all-flying tailpanes is effective only within a limited range of the fuselage angle of attack, above which acts in a reverse way, due to extensive flow separation on the element at higher local angle of attack,
- The split version of the tail surfaces is safer than the all-flying version (no reverse action), however its effectivenes also decreases rapidly above α=15°,
- Effectiveness of taiplanes at high angles of attack may be improved by changing inclination angle for manouvers at low speed, high fuselage angle of attack, such as power-off landing approach. This option is safer with the split version (stabilizer, rudder) because of the danger of reverse action of the all-flying version.

REFERENCES

[1] Fluent 6.3 User's Guide, Ansys.Inc.
[2] Menter, F. R. (1993), "Zonal Two Equation k-ω Turbulence Models for Aerodynamic Flows", AIAA Paper 93-2906.
[3] Roskam J "Airplane Flight Dynamics and Auytomatic Flight Controls", DARCoropration, Lawrence, Kansas6604, USA, 1995.
[4] Stalewski W., Zalewski W. „Analysis of aerodynamic properties of the lifting rotor and the range of attainable load factors in operational conditions of a gyroplane", Report of Institute of Aviation nr R13003_BA2-038/11 (in Polish), 2011.

JANUSZ SZNAJDER

# SKUTECZNOŚĆ USTERZENIA WIATRAKOWCA W KSZTAŁCIE ODWRÓCONEGO "V" PRZY MAŁEJ PRĘDKOŚCI I NA DUŻYCH KĄTACH NATARCIA

*Streszczenie*

*Usterzenie w układzie „V" posiada pewne zalety wobec usterzenia klasycznego, polegające głównie na prostszej konstrukcji struktury i niższych kosztach wytwarzania, przy nieco bardziej skomplikowanym mechaniźmie sterowania. Z podobnych powodów ten układ jest również atrakcyjny w projektowaniu wiatrakowców. Jednak rozważając ten układ usterzenia w projekcie wiatrakowca należy uwzględnić niektóre specyficzne czynniki dla mechaniki lotu tego typu statków powietrznych. Jednym z nich są wahania łopat wirnika, stąd bezpieczniejszym rozwiązaniem dla wiatrakowca jest układ odwróconego „V". Innym czynnikiem który należy brać pod uwagę jest zakres kątów natarcia kadłuba dla którego usterzenie musi pracować skutecznie. Jest to istotne szczególnie dla sterowania kątem odchylenia. Sterowność kierunkowa powinna być zapewniona dla warunków stromego podejścia do lądowania bez napędu przy kątach natarcia przekraczających 20° i dla warunków lądowania na niewielkiej powierzchni z wyhamowaniem prędkości postępowej przez wychylenie głowicy wirnika w tył. W pracy badano przy pomocy numerycznych symulacji opływu skuteczność dwóch alternatywnych wariantów usterzenia w układzie odwróconego „V". Analizę przeprowadzono dla opływu dwu- i trójwymiarowego. Jednym z rozwiązań było usterzenie płytowe a drugim usterzenie dzielone na statecznik i ster mające ten sam obrys co usterzenie płytowe. W obliczeniach opływu dwuwymiarowego wykazano że dla usterzenia dzielonego o cięciwie steru równej 60-70% cięciwy profilu w warunkach startu i lądowania maksymalna wartość siły nośnej jest wyższa niż dla usterzenia płytowego przy wartości pochodnej współczynnika siły nośnej względem kąta wychylenia steru tylko o 10% mniejszej od usterzenia płytowego. W obliczeniach opływu trójwymiarowego wykazano, że układ odwróconego usterzenia „V" pracuje skutecznie tylko w ograniczonym zakresie kątów natarcia, w przybliżeniu ±10-15°. Poza tym zakresem jego skuteczność raptownie spada, szczególnie w przypadku usterzenia płytowego. Dla tej konfiguracji pochodna współczynnika momentu odchylającego względem kąta wychylenia steru zmienia znak dla kątów natarcia kadłuba przekraczających 12° z powodu rozległego oderwania opływu na elemencie usterzenia zwiększającym kąt natarcia. Usterzenie dzielone nie wykazuje odwrotnego działania, jednak jego skuteczność również szybko spada na dużych kątach natarcia. Proponowanym rozwiązaniem jest wprowadzenie mechanizmu przestawiania kąta zaklinowania usterzenia dla manewrów przeprowadzanych na dużych kątach natarcia kadłuba, np. dla stromego podejścia do lądowania bez napędu. Rozwiązanie to jest bezpieczniejsze w zastosowaniu z usterzeniem dzielonym z powodu braku odwrotnego działania które mogłoby wystąpić w przypadku usterzenia płytowego.*